

WT 17024

THERMO- MECHANICAL FATIGUE BEHAVIOR OF MATERIALS

SECOND VOLUME

Michael J. Verrilli and
Michael G. Castelli
editors



STP 1263

Library of Congress Cataloging-in-Publication Data

Thermomechanical fatigue behavior of materials. Second volume /

Michael J. Verrilli and Michael G. Castelli, editors.

(STP : 1263)

Contains papers presented at the Second Symposium on Thermomechanical Fatigue Behavior of materials held 14–15 November 1994 in Phoenix, AZ"—Foreword.

"ASTM publication code number (PCN) 04-012630-30."

Includes indexes.

ISBN 0-8031-2001-X

1. Alloys—Fatigue. 2. Alloys—Thermomechanical properties.
3. Composite materials—Thermomechanical properties. 4. Fracture mechanics. I. Verrilli, Michael J. II. Castelli, Michael G.

TA483.T48 1996

620.1'617—dc20

96-19174

CIP

Copyright © 1996 AMERICAN SOCIETY FOR TESTING AND MATERIALS, West Conshohocken, PA. All rights reserved. This material may not be reproduced or copied, in whole or in part, in any printed, mechanical, electronic, film, or other distribution and storage media, without the written consent of the publisher.

Photocopy Rights

Authorization to photocopy items for internal, personal, or educational classroom use, or the internal, personal, or educational classroom use of specific clients, is granted by the American Society for Testing and Materials (ASTM) provided that the appropriate fee is paid to the Copyright Clearance Center, 222 Rosewood Drive, Danvers, MA 01923, Tel: 508-750-8400 online: <http://www.copyright.com/>.

Peer Review Policy

Each paper published in this volume was evaluated by three peer reviewers. The authors addressed all of the reviewers' comments to the satisfaction of both the technical editor(s) and the ASTM Committee on Publications.

To make technical information available as quickly as possible, the peer-reviewed papers in this publication were prepared "camera-ready" as submitted by the authors.

The quality of the papers in this publication reflects not only the obvious efforts of the authors and the technical editor(s), but also the work of these peer reviewers. The ASTM Committee on Publications acknowledges with appreciation their dedication and contribution of time and effort on behalf of ASTM.

Foreword

This publication, *Thermomechanical Fatigue Behavior of Materials: Second Volume*, contains papers presented at the Second Symposium on Thermomechanical Fatigue Behavior of Materials held 14–15 November 1994 in Phoenix, AZ. The symposium was sponsored by ASTM Committee E-8 on Fatigue and Fracture. Michael J. Verrilli, of the NASA Lewis Research Center in Cleveland, and Michael G. Castelli, with NYMA, Inc., NASA LeRC Group in Brook Park, OH, presided as symposium chairmen and are editors of the resulting publication.

Overview

Background

Virtually all high-temperature components experience service cycles that include simultaneous temperature and load cycling, or thermomechanical fatigue (TMF). Materials testing and characterization are required to capture the often unique synergistic effects of combined thermal and mechanical loading. This information can make possible the proper formulation of models used for component lifetime prediction and design, and can guide materials development.

The paper included in this volume were written in conjunction with a symposium organized to disseminate current research in the area of TMF behavior of materials. ASTM, through the members of Committee E-8 on Fatigue and Fracture, has traditionally had a keen interest in thermal and thermomechanical fatigue, as evidenced by the numerous STPs which discuss the issue. In 1968, the first ASTM paper on TMF appeared in STP 459, *Fatigue at High Temperature*. Carden and Slade discussed the behavior of Hastelloy X under strain-controlled isothermal and TMF conditions. *The Handbook of Fatigue Testing* (STP 566, published in 1974) described a technique for thermal fatigue testing of coupon specimens as well as the structural TMF test system for the airframe of the Concorde. STP 612, *Thermal Fatigue of Materials and Components* (1975) is the proceedings of the first comprehensive ASTM symposium on thermal and thermomechanical fatigue. Paper topics included TMF test techniques, life prediction methods, and TMF behavior of advanced materials such as ceramics and directionally-solidified superalloys. A symposium entitled "Low Cycle Fatigue" (STP 942) held in 1988 contained five papers on thermal and thermomechanical fatigue. TMF test techniques, deformation behavior and modeling, and observation of microstructural damage were presented. The first ASTM STP devoted to TMF of materials (and the predecessor to this volume) was the proceedings of the 1991 symposium on *TMF Behavior of Materials* (STP 1186). Several papers discussed the role of environmental attack on performance and life modeling of high-temperature alloys subjected to TMF loadings. In addition, this STP contains two papers which discuss TMF of metal matrix composites, an indication of the emerging interest in this class of materials for high-temperature applications.

ASTM is also actively pursuing development of a standard practice for TMF testing. Numerous standard practices for isothermal low-cycle fatigue testing exist (including ASTM E606 for strain-controlled testing and E466 for load-controlled testing), but none exist for TMF. However, the first standard for strain-controlled TMF testing of metallic materials is under development by an ISO working group in conjunction with ASTM Committee E-8 on Fatigue and Fracture. We expect that the resulting international standard will be the foundation of an ASTM standard.

Summary of the Papers

High-Temperature Structural Alloys

Most papers in this section discuss high-temperature alloys used for gas turbine engines, such as Ni-base superalloys and titanium alloys. Steels which are subjected to TMF conditions in power generation applications are discussed as well. The topics of the papers in this section on TMF behavior of high-temperature alloys include crack initiation and growth,

novel experimental techniques, deformation modeling, and the role of coatings on life and microcracking.

Chataigner and Remy studied the TMF behavior of a chromium-aluminum coated [001] single crystal using a diamond-shaped strain-temperature cycle. They found no difference between the lives of coated and bare specimens. A life prediction model based on microcrack propagation due to fatigue and oxidation damage is evaluated.

Kraft and Mughrabi examined the crack evolution and microstructural changes of a single-crystal superalloy subjected to in-phase, out-of-phase, and diamond TMF cycle types. The morphology of the γ' structure after TMF cycling was found to be dependent on cycle type. The maximum tensile stress response of the [001] oriented specimens governed life for all the cycle types.

Meyer-Olbersleben et al. performed thermal fatigue (TF) experiments on blade-shaped, wedge specimens made of single-crystal superalloys. They proposed an “integrated” approach where the temperature-strain history measured during TF experiments is used as the basic cycle for a TMF investigation. This method is suggested as an alternative to finite element calculations to deduce the stress history of wedge specimens.

Bressers, Martínez-Esnaola, Timm, and co-workers contributed three papers examining the role of a coating on the TMF behavior of single-crystal Ni-base superalloys. In the first contribution, Bressers et al. studied the effect of TMF cycle type on the lives of a coated and uncoated single-crystal superalloy. This study reports the various modes of crack initiation, crack growth, and the stress and inelastic strain response due to in-phase cycle and -135° lag cycle. For uncoated specimens, the cycle type significantly affected the mode of crack initiation. Also, life debits due to the presence of the coating varied as a function of strain range and cycle type. In the second paper by this group, Martínez-Esnaola et al. investigated cracking of the coating on the Ni-base single crystals subjected to the -135° lag TMF cycle. The mode of coating crack initiation depended on the applied mechanical strain range, while crack initiation of bare specimens occurred via a single mode. A fracture mechanics model was applied to examine the effects of parameters such as coating thickness and temperature on the coating toughness, strain to cracking, and crack density. In the third contribution, Bressers et al. used a crack shielding model in an effort to explain the experimentally-observed debit in TMF life due to the presence of the coating on the single-crystal specimens. Higher crack-growth rates of the main crack were observed in coated specimens relative to the uncoated material. The crack shielding model was used in a parametric study to stimulate the growth of interacting, parallel cracks. The results of the analysis indicated that crack shielding effects due to the presence of the coating did not play a primary role in the life difference, and that other factors should be investigated as the potential cause, such as presence of residual stresses or thermal expansion mismatch of the coating and substrate.

Two papers discussed TMF of stainless steels. Zamrick and his co-workers compared the TMF and high-temperature LCF behavior of type 316 stainless steel. Yamauchi et al. conducted structural thermal fatigue tests on tubes of 304 stainless steel to simulate the service conditions. A FEM stress analysis revealed the stress state and temperature-strain phasing for the inner and outer surfaces of the pipe which experienced through-thickness gradients during the tests. The analysis, combined with uniaxial specimen tests, explained the experimentally-observed difference of crack initiation life between the inner and outer surfaces.

Arnold et al. present their recent developments in viscoplastic deformation modeling. The model utilizes an evolutionary law that has nonlinear kinematic hardening and both thermal and strain-induced recovery mechanisms. One tensorial internal state variable is employed. A unique aspect of the present model is the inclusion of nonlinear hardening in the evolution law for the back stress. Verification of the proposed model is shown using non-standard

isothermal and thermomechanical deformation tests on a titanium alloy commonly used as the matrix in SiC fiber-reinforced composites.

A novel test method to assess the role of temperature in determining the operative fracture mode and crack growth rates in superalloy single crystals is presented in the paper by Cunningham and DeLuca. The technique involves varying temperature with crack length according to a user-supplied function and was shown to work with several specimen geometries. Applications of the test method for screening of temperature-dependent crack growth behavior and model verification are discussed.

Gao et al. describe a unique thermal fatigue test rig fitted with a chamber that enables testing under various environments, including flowing hydrogen. The performance of the rig and the associated test procedures were evaluated through experimental testing of a γ TiAl alloy.

Dai et al. discuss thermal mechanical fatigue crack growth (TMFCG) results obtained for two titanium alloys. Tests were conducted using several strain-temperature phasings, and the ability of several fracture mechanics parameters to correlate the data was evaluated. Also, a model to predict TMFCG rates is presented and its application to estimate lives of engine components is discussed.

Titanium Matrix Composites

Over the past several years, silicon-carbon-fiber-reinforced titanium matrix composites (TMCs) have received considerable attention in the aeronautics and aerospace research communities for potential use in advanced high-temperature airframe and propulsion system applications. The obvious attractions of TMCs are the high stiffness and strength-to-weight ratios achievable at elevated temperatures, relative to current generation structural alloys. The papers included in the TMC section of this publication discuss many of the complex phenomenological behaviors and analytical modeling issues which arise under TMF loading conditions.

Coker et al. present a deformation analysis of a [0/90] TMC. A micromechanics approach is taken which treats the crossply as a three-constituent material consisting of a linear-elastic [0] fiber, a viscoplastic matrix in the [0] ply, and a viscoplastic [90] ply with damage to simulate fiber/matrix (f/m) interface separation. The authors clearly show the importance of treating the TMC as a thermoviscoplastic medium and the need to account for f/m separation when assessing [0/90] crossply macroscopic response. The contribution by Roberston and Mall features a modified Method of Cells micromechanics approach coupled with a unique f/m interface failure scheme based upon a probabilistic failure criterion. The proposed methodology incorporates the effects of both normal and shear f/m interface failures. Verification of the analysis is conducted under TMF loadings where the model appears to capture the progression of the interfacial damage with cycles.

Johnson et al. present a detailed experimental evaluation of the fatigue behavior of a [0/90] TMC subjected to a generic hypersonic flight profile. Material response under isolated segments of the flight profile are also examined to help identify critical combinations of load and time at temperature. Results indicate that sustained load at temperature had a more deleterious effect on fatigue life than that of a combined nonisothermal temperature profile and mechanical loading. Significant strain accumulations and eventual failure of the composite under sustained load conditions were found to result primarily from [90] f/m interface separation and sustained load crack growth, rather than more traditional creep mechanisms such as viscoplastic deformation of the matrix. Aksoy et al. also examine the fatigue performance of a TMC subjected to a mission cycle, but here the cycle was designed to simulate

the stress-temperature-time profile in a TMC ring reinforced impeller of a turboshaft engine. Results indicate that although the 14-minute mission cycle life was found to be significantly less than that revealed under isothermal conditions at a much faster loading rate (as expected), the failure mechanisms appeared to be very similar.

The paper contributed by Neu extends the concept of mechanistic maps to TMCs and presents unique TMF damage mechanisms maps for unidirectional laminates loaded in the fiber direction. Extensive experimental data and observations are weighted to guide the use of adopted and derived life prediction models and specify mechanistic regions of the maps. Combined life and damage mechanism maps are then constructed over a wide range of stress and temperature using the characterized prediction models. Ball presents experimental results on both [0] and [0/90] TMCs, along with a continuum damage-mechanics-based lifing approach. Damage is incorporated into the material constitutive equations at the ply level prior to the use of classical lamination theory to obtain the laminate response. Three types of damage are considered, including fiber breakage, f/m debonding, and matrix microcracking.

Nicholas and Johnson present a systematic study of the potential interactions between cyclic fatigue and creep (superimposed hold times) in [0] and [0/90] TMCs. Cyclic conditions involving low-frequency cycling and/or hold times at relatively high temperatures were found to result in failures dominated by time-dependent mechanisms with little or no contribution from fatigue-induced failure mechanisms. This observation was elucidated through a linear damage summation model which treats cycle- and time-dependent mechanisms separately. Blatt et al. also employ a linear summation model, but here in the context of understanding and predicting fatigue crack growth (FCG) rates. A unique study is presented examining the FCG behavior of a unidirectional TMC under TMF conditions. Results indicate that the amount of cycle time spent at or near T_{\max} conditions was a key factor influencing the FCG rate. The proposed model appeared to be successful at predicting the FCG rate of a proof test involving a continually changing temperature and load range to produce a constant FCG rate.

Concluding Remarks

We feel that the work presented here is an outstanding reflection of the latest research in this demanding field and a noteworthy contribution to the literature. The contributions from both U.S. and international authors give a global perspective of the concerns and approaches. Finally, we would like to express our gratitude to the authors, reviewers, and ASTM staff for their hard work and resulting contributions to this STP.

Michael J. Verrilli

Symposium co-chairman and co-editor;
NASA Lewis Research Center, Cleveland,
Ohio.

Michael G. Castelli

Symposium co-chairman and co-editor;
NYMA, Inc., NASA LeRC Group, Brook
Park, Ohio.

Contents

Overview—M. J. VERRILLI AND M. G. CASTELLI

HIGH-TEMPERATURE STRUCTURAL ALLOYS

Thermomechanical Fatigue Behavior of Coated and Bare Nickel-Based Superalloy Single Crystals—E. CHATAIGNER AND L. REMY 3

Thermomechanical Fatigue of the Monocrystalline Nickel-Based Superalloy CMSX-6—S. KRAFT AND H. MUGHRABI 27

On Thermal Fatigue of Nickel-Based Superalloys—F. F. MEYER-OLBERSLEBEN, C. C. ENGLER-PINTO, JR., AND F. RÉZAI-ARIA 41

Effects of Cycle Type and Coating on the TMF Lives of a Single Crystal Nickel-Based Turbine Blade Alloy—J. BRESSERS, J. TIMM, S. WILLIAMS, A. BENNETT, AND E. AFFELDT 56

Crack Initiation in an Aluminide Coated Single Crystal During Thermomechanical Fatigue—J. M. MARTÍNEZ-ESNAOLA, M. ARANA, J. BRESSERS, J. TIMM, A. MARTÍN-MEIZOSO, A. BENNETT, AND E. AFFELDT 68

Coating Effects on Crack Growth in a Single Crystal Nickel-Based Alloy During Thermomechanical Fatigue—J. BRESSERS, J. M. MARTÍNEZ-ESNAOLA, A. MARTÍN-MEIZOSO, J. TIMM, AND M. ARANA-ANTELO 82

✓ **Isothermal and Thermomechanical Fatigue of Type 316 Stainless Steel**—S. Y. ZAMRIK, D. C. DAVIS, AND L. C. FIRTH 96

Thermal Fatigue Behavior of SUS304 Pipe Under Longitudinal Cyclic Movement of Axial Temperature Distribution—M. YAMAUCHI, T. OHTANI, AND Y. TAKAHASHI 117

Assessing Crack Growth Behavior Under Continuous Temperature Gradients—S. E. CUNNINGHAM AND D. P. DELUCA 130

A Fully Associative, Nonisothermal, Nonlinear Kinematic, Unified Viscoplastic Model for Titanium Alloys—S. M. ARNOLD, A. F. SALEEB, AND M. G. CASTELLI 146

500-163

Thermal Fatigue Testing System for the Study of Gamma Titanium Aluminides in Gaseous Environments—M. GAO, W. DUNFEE, C. MILLER, R. P. WEI, AND W. WEI	174
✓ Thermal Mechanical Fatigue Crack Growth in Titanium Alloys: Experiments and Modeling—J. DAI, N. J. MARCHAND, AND M. HONGO	187
TITANIUM MATRIX COMPOSITES	211
Analysis of the Thermoviscoplastic Behavior of [0/90] SCS-6/TIMETAL® 21S Composites—D. COKER, R. W. NEU, AND T. NICHOLAS	213
Analysis of the Thermomechanical Fatigue Response of Metal Matrix Composite Laminates with Interfacial Normal and Shear Failure—D. D. ROBERTSON AND S. MALL	236
Damage Accumulation in Titanium Matrix Composites Under Generic Hypersonic Vehicle Flight Simulation and Sustained Loads—W. S. JOHNSON, M. MIRDAMADI, AND J. G. BAKUCKAS, JR.	252
Fatigue Behavior of [0]8 SCS-6A1/TI-6-4V Composite Subjected to High Temperature Turboshift Design Cycles—S. Z. AKSOY, J. GAYDA, AND T. P. GABB	266
Thermomechanical Fatigue Damage Mechanism Maps for Metal Matrix Composites—R. W. NEU	280
An Analytical and Experimental Investigation of Titanium Matrix Composite Thermomechanical Fatigue—D. L. BALL	299
Time- and Cycle-Dependent Aspects of Thermal and Mechanical Fatigue in a Titanium Matrix Composite—T. NICHOLAS AND D. A. JOHNSON	331
Modeling the Crack Growth Rates of a Titanium Matrix Composite Under Thermomechanical Fatigue—D. BLATT, T. NICHOLAS, AND A. F. GRANDT, JR.	352
Author Index	371
Subject Index	373

High-Temperature Structural Alloys

Eric Chataigner and Luc Remy *

THERMOMECHANICAL FATIGUE BEHAVIOUR OF COATED AND BARE NICKEL-BASED SUPERALLOY SINGLE CRYSTALS

REFERENCE: Chataigner, E. and Remy, L., "**Thermomechanical Fatigue Behaviour of Coated and Bare Nickel-Based Superalloy Single Crystals,**" *Thermomechanical Fatigue Behavior of Materials: Second Volume*, ASTM STP 1263, Michael J. Verrilli and Michael G. Castelli, Eds., American Society for Testing and Materials, 1996.

ABSTRACT: The thermal-mechanical fatigue behaviour of chromium-aluminium coated [001] single crystals of AM1, a nickel-base superalloy for turbine blades, is studied using a "diamond" shape cycle from 600° to 1100°C. Comparison with bare specimens does not show any significant difference in thermal-mechanical fatigue nor in isothermal low cycle fatigue at high temperature. Metallographic observations on fracture surfaces and longitudinal sections of specimens tested to fatigue life or to a definite fraction of expected life have shown that the major crack tends to initiate from casting micropores in the sub-surface area very early in bare and coated specimens, under low cycle fatigue or thermal-mechanical fatigue. But the interaction between oxidation and fatigue cracking seems to play a major role. A simple model proposed by Reuchet and Rémy has been identified for this single crystal superalloy. Its application to the life prediction under low cycle fatigue and thermal-mechanical fatigue for bare and coated single crystals with different orientations is shown.

KEYWORDS: thermomechanical fatigue, nickel-based superalloy, single crystals, coatings, lifetime prediction.

INTRODUCTION

Cooled turbine blades in jet engines must have a good resistance to thermal-mechanical cyclic loadings due to the superposition of centrifugal loads and thermal stresses

* Centre des Matériaux P.M. FOURT E.N.S.M.P. URA 866 - B.P. 87 91003 EVRY Cedex (FRANCE)

during take-off and landing operations. These components have been designed for a long time using simply isothermal low cycle fatigue (LCF) and creep tests. However the synergy between fatigue damage and time dependent phenomena, such as creep or oxidation, can be much stronger under thermal transient conditions than under isothermal creep fatigue loading. Thermal-mechanical fatigue (TMF) therefore is especially appropriate to simulate the behaviour of critical areas of components.

The advantages and limitations of the TMF test have been discussed in various places [1-3]. There is no temperature gradient across the specimen section and the stress is induced by a mechanical strain which is applied to the specimen to simulate the constrained thermal expansion of a component part. The major limitation is that to avoid temperature gradient in the section, cycle periods can be rather longer than thermal transients in actual components.

In TMF testing, the phasing of strain and temperature can be arbitrarily varied. Most authors have used two basic mechanical strain versus temperature cycles : the "in-phase" cycle where the mechanical strain is maximum at maximum temperature and the "out-of-phase" cycle where the mechanical strain is maximum at the minimum temperature [4-6]. The phasing of strain and temperature can vary to a great extent according to component geometry, engine type and so on. In our group, realistic simulation type cycles are preferred which often have a large hysteresis and simulate more closely conditions experienced in service [1, 7].

Turbine blades are generally made from cast superalloys. Though both creep and oxidation can interact with fatigue in the so-called creep-fatigue tests or TMF tests, superalloys are very susceptible to oxidation effects. This has been emphasized by Coffin [8] and by later authors [9-11]. Various damage models have been proposed to account for the interaction between oxidation and fatigue in these alloys [9, 12, 13, 14].

Directionally solidified single crystals are now introduced in advanced engines to increase performance. Nickel-based superalloy single crystals have better creep resistance, much higher thermal fatigue resistance and higher incipient melting temperatures than conventionally cast alloys [15-17]. They are cast with the [001] direction of the face-centered cubic (fcc) lattice of the matrix along the main direction of the blade.

Turbine blades in jet engines are exposed to oxidation and corrosion from hot combustion gas. The intrinsic resistance of cast superalloys to oxidation and corrosion is not high enough and coatings are generally applied on components to protect them from the corrosive environment. Aluminide coatings in particular are widely used owing to their good resistance to oxidation.

We have recently completed a detailed study of the behaviour of bare AM1 single crystals, which is a new superalloy used by SNECMA for advanced blades, under LCF and under TMF conditions [18, 19]. Coating alloys to protect turbine engine hot section airfoils have been developed by SNECMA with a low activity chromizing-aluminising vapor process referred to as CIA in the following. The purpose of the present work was twofold : firstly to investigate the TMF behaviour of chromium-aluminium coated AM1 nickel base superalloy single crystals with a [001] orientation, using the same TMF cycle as for the bare alloy from 600°C to 1100°C (873K to 1373K); secondly to evaluate life predictions from a simple engineering model for different loading cycles (LCF, TMF), for different orientations of the loading axis, either in the bare or coated condition.

This paper reports the results obtained on AM1 single crystals with a [001] orientation which have been coated by the C1A chromising-aluminising process under TMF and conventional LCF tests at 950°C (1223K) and 1100°C (1373K). Their behaviour is compared with that of bare specimens and metallographic observations of coated samples are then described. An oxidation-fatigue damage model which has been previously proposed to predict the lifetime under LCF at high temperatures and TMF cycling for conventionally cast superalloys is recalled and its application of to superalloy single crystals is described. Predictions of this model are finally compared with various results on bare and coated AM1 single crystals with different orientations.

EXPERIMENTAL PROCEDURE

The composition of the alloy used in this study is given in Table I.

TABLE I--Chemical composition of the various batches of AM1 used (weight %).

	Ni	Ta	Cr	Co	W	Al	Mo	Ti
Batch JA 81731	63.8	7.9	7.7	6.5	5.7	5.2	1.9	1.1
Batch JA 81512	63.2	8.2	7.9	6.6	5.6	5.2	2.1	1.2
Batch RA 14684	63.2	8.3	7.6	6.4	5.4	5.5	2.1	1.3

Three alloy batches were used JA81731, JA81512 and RA14684. The last batch was used mostly for the study of the C1A coated samples. Specimens were in the form of cast cylinders 20 mm in diameter and 120 mm in length. These cylindrical bars were cast with their main axis along the [001] dendritic solidification direction, in this study. The first two batches were studied in the bare condition and were given a solution heat treatment at 1300°C for 3 hours, a precipitation heat treatment at 1100°C for 10 hours and a final ageing heat treatment at 870°C for 16 hours. The microstructure is composed by a distribution of γ precipitates in a (fcc) matrix. Their size and volume fraction were approximately 0.45 μm and 68 pct, respectively. The third batch was studied in the bare and coated conditions and was given an industrial heat treatment. This comprises the chromising and aluminising treatment which amounts to 15 h at 1050 °C and was optimised to give the same distribution of γ precipitates as in the first two batches.

Hollow cylindrical specimens with 1mm wall thickness, 11mm external diameter and 25mm gauge length were used for TMF tests. This shape, shown on Fig 1, allowed to obtain a uniform temperature distribution in the radial direction. LCF specimens were solid and cylindrical, 12 mm in gauge length and 6 mm in diameter. After machining and before mechanical testing, bare specimens were polished down to 3 μm grade diamond paste. The inner surface of TMF specimens was polished with a special tool in order to avoid crack initiation at machining scratches.

The crystallographic orientation of specimens was checked using the Laue back reflection X-ray diffraction technique. Most specimens were within 5 degrees of their nominal orientation.

All the LCF tests were conducted under symmetrical ($R_\epsilon = -1$) total axial strain control on a screw-driven machine. The wave shape was triangular with a frequency of 0.05 Hz and tests were made at 950 and 1100°C.

The objective of the TMF test is to simulate the behaviour of critical parts of components. In this thermal-mechanical fatigue test, there is no temperature gradient across the specimen section and the stress is induced by a mechanical strain to simulate

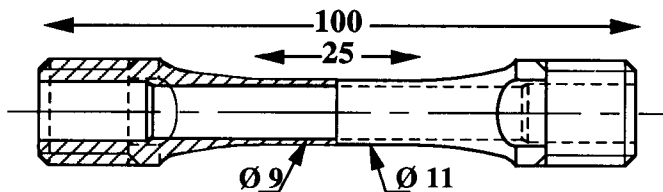


Figure 1 : TMF specimen geometry.

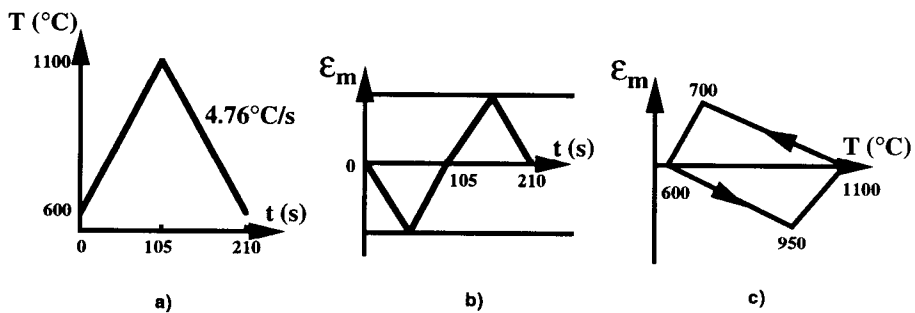


Figure 2 : Thermal-mechanical fatigue cycle:

- a) Temperature versus time diagram,
- b) Mechanical strain versus time diagram,
- c) Mechanical strain versus temperature diagram.

the constrained thermal expansion, due to temperature gradients across the components section. The TMF tests were performed using a specific cycle presented on Fig. 2 which simulates thermal loading conditions experienced in service at the leading edge of a blade in a jet engine and was used in a previous investigation in the bare condition [19]. A mechanical strain-temperature loop was used from 600° to 1100°C (873 to 1373K) with peak strains at intermediate temperature : 950°C (1223K) in compression on heating and 700°C (973K) in tension on cooling.

Our own TMF test facilities used a micro-computer to generate two synchronous temperature and mechanical strain signals and a lamp furnace to heat the sample, as described in earlier publications [2, 3]. Thermal cycling time is 210 s. During the test, temperature is also measured by a coaxial thermocouple located and attached on the cylindrical part.

Smooth specimen testing is especially appropriate to investigate the life to engineering crack initiation. Crack growth was monitored using the d.c. potential drop technique in all the specimens and the plastic replication technique in some specimens. This second procedure which necessitates test interruptions, enabled cracks as small as 10µm in surface length to be detected by scanning electron microscopy (SEM). Specimens were sectioned and broken in order to get an experimental calibration curve between surface crack length " a_s " and crack depth " a_p ". Surface cracks observed in different TMF specimens with a depth in the range 0.05 to about 0.8mm have a semi-elliptical shape. Experimental a_s and a_p data can be fitted by the equation $a_p = 0.38 a_s$ using a least square method, as previous LCF data on the same alloy [18] as well as on other single crystal alloys [20]. For coated specimens, tests were conducted too up to different fractions of expected life and the crack distribution was observed on longitudinal sections by SEM.

Tests were stopped when the major crack grows through wall thickness or slightly before 1mm depth (this corresponds to our definition of N_f). Previous work on solid LCF specimens [10, 11] has shown that using a potential drop technique, a conventional fatigue life can be defined to 0.3mm crack depth, referred to as N_i . Consistent fatigue lives are thus given by solid and hollow specimens under LCF and N_i data under TMF and LCF can be reliably compared. In order to describe more closely the initiation phase and to trigger differences between coated and bare specimens, data to 0.1mm (referred to as N_e) were also estimated whenever possible.

RESULTS

Cyclic Stress-Strain Behaviour under TMF

Stepwise-increasing strain TMF tests were carried out on coated [001] specimens. Fig. 3 shows the variation of stress as a function of mechanical strain. On this kind of material, with a symmetrical strain range imposed, the hysteresis loops are stabilized after a few cycles. The stress-mechanical strain response in non-isothermal conditions is not usual and necessitates some comments. Because the material behaviour is different at the temperature of each peak strain, the inelastic strain is mostly created during the heating phase in compression. Though strain cycling was fully reversed, the stress cycle is unbalanced with a positive tensile mean stress. The particular shape of the TMF hysteresis loops is the result of the combined variations of elastic modulus E , monotonic yield strength σ_y and imposed mechanical strain ϵ_m with temperature T . A crystallographic model has been recently proposed which uses viscoplastic constitutive equations at the level of the slip system considering both cube and octahedral slip planes

[21]. This model describes the stress-strain loop as well as the active slip systems of AM1 single crystals under isothermal conditions [21] and was shown to predict quite accurately the present stress-strain loops under TMF [22].

TMF and LCF Life of Bare and Coated Specimens with a [001] Crystallographic Orientation

Test results--TMF life results for 1 mm crack depth (N_f) of the [001] specimens are plotted versus the total mechanical strain range in the bare condition (Fig. 4). There is no significant difference between the different batches of material. The endurance of coated specimens is almost the same as that of bare specimens for the TMF cycle used (Fig. 5).

The life to engineering crack initiation in the bare condition is mostly spent in micro-crack growth as shown by the variation of crack depth, which has been deduced from the observations of plastic replicas, versus the fraction of total life (Fig.6). Cracks a few tens μm in depth can be actually detected within about 5 pct of total life. Whatever the mechanical strain range, cracks propagated in stage II mode, i.e. mode I opening, from the initiation site to 0.4mm about. But when cracks are longer they deviated and tend to follow a crystallographic path, with a higher crack growth rate. Contrarily to LCF data [18], short TMF lives do not seem to fit the straight line for longer lives as a function of mechanical strain range.

The observations of interrupted tests after some fraction of expected life has shown that a major crack initiates quite early in the TMF life of coated specimens (see for instance Fig.6). The endurance of chromaluminized (C1A coated) specimens tested in LCF at 950°C at a frequency of 0.05 Hz is compared with that of bare samples under the same test conditions using a total mechanical strain range in Fig.7. There is no noticeable difference within the experimental scatter.

The life of chromaluminized specimens under TMF is compared with that under LCF at 950 and at 1100 °C versus total mechanical strain range and versus stress range in Figs. 8a and 8b respectively. The TMF life versus stress range is in pretty good agreement with LCF life at 950°C. With the total mechanical strain range, TMF life is well described by LCF life at 1100°C.

Metallographic observations--The damage mechanisms of AM1 single crystals under TMF cycling of different orientations were recently reported in the bare condition [19] and can be summarised as follows : at high strain ranges, the major crack nucleates from a large casting micropore at the surface or in the subsurface area; at low strain ranges, the major crack nucleates from oxidised areas at the surface.

The major crack seems always to initiate at a subsurface casting micropore beneath the coating layer from the observation of fracture surfaces of coated [001] specimens tested in LCF at 950°C. Fig. 9 shows that the main crack looks as a surface initiated crack despite this crack initiation mechanism. Numerous cracks actually form in the coating but they stop at the interface between coating and substrate and do not grow into the substrate. At the lower strain ranges, the crack initiation mechanism seems unaltered but the cracks are much more oxidised (Fig. 10); localised oxidation occurs at the interface between coating and substrate.

Under TMF cycling, the fracture surfaces of coated [001] specimens tested at high strain ranges, look like those tested in LCF at 950°C, Fig.11 and the major crack initiates at a subsurface casting micropore. At low strain ranges, the initiation mechanisms of the